# Could the 650 GeV Excess be a Pseudoscalar of a 3-Higgs Doublet Model?

Ayoub Hmissou
*Laboratory of Theoretical and High Energy Physics,Faculty of Science, Ibnou Zohr University, B.P 8106, Agadir, Morocco.*

Stefano Moretti
*School of Physics & Astronomy, University of Southampton, Southampton, SO17 1BJ, United Kingdom and Department of Physics & Astronomy, Uppsala University, Box 516, SE-751 20 Uppsala, Sweden.*

Larbi Rahili
*Laboratory of Theoretical and High Energy Physics, Faculty of Science, Ibnou Zohr University, B.P. 8106, Agadir, Morocco.*

(Dated: Version 5.0 – September 9, 2025)

In this study, we propose the interpretation of a 650 GeV excess observed at the Large Hadron Collider (LHC) by the CMS Collaboration in terms of the production of a CP-odd (or pseudoscalar) Higgs boson $A$, with mass around 650 GeV, decaying into the Standard Model (SM)-like Higgs state $h_{125}$ (in turn decaying into $\gamma\gamma$) and a $Z$ boson (in turn decaying into $b\bar{b}$), within a 3-Higgs Doublet Model (3HDM) featuring two active and one inert doublet, known as the I(1+2)HDM. This theoretical structure features a spectrum with both the SM-like Higgs boson (with a 125 GeV mass) and a lighter CP-even (or scalar) Higgs state with mass around 95 GeV, $h_{95}$, which is present in this scenario for the purpose of simultaneously explaining anomalies seen in the $b\bar{b}$, $\gamma\gamma$ and $\tau^+\tau^-$ final states in searches for additional light Higgs states at the Large Electron-Positron (LEP) collider and LHC itself. It should be noted that, in the I(1+2)HDM, the inert sector presents loop-induced enhancements to the $h_{95} \to \gamma\gamma$ width via inert charged Higgs states, providing a viable mechanism to explain, in particular, the observed (and most significant) di-photon excess at 95 GeV. Taking into account both experimental and theoretical constraints, our results can not only explain the aforementioned anomalies (possibly, aside from the $\tau^+\tau^-$, which is the most marginal one) but also predict, as collateral signals, resonant production of the same CP-odd scalar $A$ followed by the decays: (i) $A \to h_{95}\, Z$, leading to the same $\gamma\gamma b\bar{b}$ final state displaying the original 650 GeV anomaly and (ii) $A \to t\bar{t}$, leading to a well-known and studied signature. Both of these signals are potentially explorable at Run 3 of the LHC and most possibly so at the High-Luminosity LHC (HL-LHC), while being consistent with current data at a significance level of $2.5\sigma$.



## I. INTRODUCTION

The discovery of a Higgs boson with a mass of 125 GeV by the ATLAS [1] and CMS [2] Collaborations marked a triumph for the Standard Model (SM) of particle physics and has opened the door to precision Higgs physics, while at the same time motivating searches for additional (psudo)scalar states Beyond the SM (BSM). Intriguingly, several experimental hints of BSM physics have emerged in recent years, notably, a local excess near 95 GeV in the $b\bar{b}$ channel at the Large Electron-Positron (LEP) collider as extracted by all Collaborations therein (ALEPH, DELPHI, L3, and OPAL) [3–5] plus in the $\gamma\gamma$ and $\tau^+\tau^-$ decay modes at the LHC as seen by CMS [6, 7] and ATLAS [8][9]. Recently, a CMS search has further reported an excess in events featuring a di-photon and a bottom quark pair (i.e., a $\gamma\gamma b\bar{b}$ final state), which could indicate a heavier resonance $X$ with a mass of approximately 650 GeV decaying into a secondary object $Y$ with a mass in the range of 90–100 GeV and the SM-like Higgs boson. Such an anomaly was observed with a local excess of $3.8\sigma$ and the best-fit value given for the cross section of this excess $\gamma\gamma b\bar{b}$ final state was as follows [10]:

$$\sigma(pp \to X_{650} \to h_{125}Y \to \gamma\gamma b\bar{b}) = 0.333^{+0.17}_{-0.13}\ (\text{fb}). \quad (1)$$

Such anomalies, although not yet conclusive in terms of significance individually, taken together, actually stand out as compelling candidates for new phenomena, and their collective persistence motivates the search for theoretical frameworks that can simultaneously explain them all.

Extensive theoretical work has been devoted to explaining the observed excesses around 95 GeV. These include non-supersymmetric models such as the 2-Higgs Doublet Model (2HDM) [11–14], its singlet (Next-to-2HDM (N2HDM)) and triplet extensions [15–20], the Georgi-Machacek (GM) model [21–23], the 3HDM containing one inert doublet (or I(1+2)HDM) [24] as well as supersymmetric frameworks such as the Next-to-Minimal Supersymmetric SM (NMSSM) [5, 25–31] and the so-called $\mu\nu$SSM [32]. Meanwhile, the anomaly observed around 650 GeV has also attracted attention and has been investigated within some BSM scenarios, including the NMSSM [33] and 2HDM [34].

In this paper, we examine yet another possibility to explain the 650 GeV anomaly, by using as a theoretical scenario the one of [24]: i.e., the I(1+2)HDM. In fact, in

doing so, we seek simultaneously a solution to the 95 GeV anomalies. As seen in [24], the advantage of this BSM framework is that it provides an additional inert charged (pseudo)scalar pair which enhances the one-loop decay into two photons of the lightest CP-even Higgs state, $h_{95}$, thereby relieving the tension existing in the 2HDM Type-I when attempting to maximise simultaneously the $b\bar{b}$, $\gamma\gamma$ and $\tau^+\tau^-$ decay rates [14]. In fact, the I(1+2)HDM that we use here is of Type-I, just like in Ref. [24]. Herein, we assume that the $X_{650}$ is the pseudoscalar Higgs state, $A$, with a mass of 650 GeV, decaying into the SM-like Higgs boson $h_{125}$ and a $Z$ boson, followed by the subsequent decays $h_{125} \to \gamma\gamma$ and $Z \to b\bar{b}$, respectively. In particular, we are suggesting that the observed $b\bar{b}$ pair originates from a $Z$ boson decay, which would then take the place of the corresponding decay of the lightest Higgs boson with a mass around 95 GeV (the one used in the NMSSM explanation), indeed, like in Ref. [34].

Notice that this interpretation is well motivated. In fact, although the CMS analysis [10] originally models the excess as a decay $X_{650} \to h_{125}Y_{95}$, with $Y_{95}$ being a spin-0 state, at $\sqrt{s} = m_A \simeq 650$ GeV, where $m_Z^2/s \ll 1$, the equivalence theorem ensures that the psudoscalar polarisation of the $Z$ boson behaves like the corresponding neutral Goldstone mode, with deviations suppressed by $\mathcal{O}(m_Z^2/s) \lesssim 2\%$. Hence, also considering the limited mass resolution of $b\bar{b}$ pairs, of some 10 GeV or so, and the fact that none of the selection cuts used by CMS has a marked spin dependence, it is conceivable that the $Z$ boson of the SM is behind the 95 GeV component of the 650 GeV anomaly.

Additionally, while assuming this excess, one should bear in mind that the $\tau^+\tau^-b\bar{b}$ channel serves as a valuable complementary probe of the same underlying dynamics. Notably, CMS has performed a dedicated search for heavy resonances in this final state, setting a 95% Confidence Limit (CL) upper limit of approximately 3 fb on the cross section $\sigma(pp \to X_{650} \to \tau^+\tau^-b\bar{b})$ [35], which would then constrain the $pp \to A \to h_{125}Z$(or $Zh_{125}Z \to \tau^+\tau^-b\bar{b}$ processes in our I(I+2)HDM. We have thus verified that the parameter space of the I(1+2)HDM, providing the illustrated explanation to all discussed anomalies, is also compliant with the aforementioned limit. The generated parameter space points were further tested against the most recent CMS upper limits on the cross section for the process $pp \to Y(\to \tau^+\tau^-)H(\to \gamma\gamma)$ [36] and these were found to constrain significantly the I(1+2)HDM parameter space (see below). Further bearing in mind [37] alongside [36], the following production and decay patterns were also subject to scrutiny: $pp \to h_{125}(\to b\bar{b})Y(\to \gamma\gamma)$ and $pp \to h_{125}(\to \tau^+\tau^-)Y(\to \gamma\gamma)$. However, given that for our solution we have $Y \equiv Z$ [38], the (non-resonant) *transition* $Z^* \to \gamma\gamma$ is highly suppressed because of the Landau-Yang theorem [39, 40] (note also Ref. [41]), the corresponding experimental limits quoted by CMS are irrelevant to our theoretical scenario (so we ignore these in the remainder).

Finally, in order to test our theoretical hypothesis, we also make predictions for two additional processes that would emerge over the same parameter space of the I(1+2)HDM, explaining all the aforementioned anomalies, both of which may be testable at the present and/or future stages of the LHC. These are the channels $pp \to A \to h_{95}\,Z$ and $pp \to A \to t\bar{t}$.

The layout of the paper is as follows. In Section II, we briefly review the main features of the I(1+2)HDM, along with the considered experimental and theoretical constraints. In Section III we present our main results by illustrating the correlations among Higgs boson masses and production cross sections relevant to searches for additional heavy resonances in various final states. In the last section, we summarise our findings.

## II. MODEL SETUP AND CONSTRAINTS

In this section, we outline the I(1+2)HDM model, which includes a scalar Dark Matter (DM) candidate. We begin with a recap of the scalar potential and the theoretical and experimental constraints affecting it. Next, we provide an analytical explanation for the $\gamma\gamma b\bar{b}$ excess within this model framework.

### A. I(1+2)HDM Basics

The I(1+2)HDM model is composed of two active Higgs doublets and one inert doublet. The extension of the SM adding only one extra Higgs doublet has been widely studied, with the 2-Higgs-doublet model (2HDM) being one of the most explored frameworks for such an extension [42]. The I(1+2)HDM discussed in Refs. [43, 44] and adopted here features a discrete $\mathbb{Z}_2 \times \mathbb{Z}_2'$ symmetry, where the $\mathbb{Z}_2$ symmetry is enforced upon the inert doublet, meaning that only the inert field $\eta$ transforms as $\eta \to -\eta$, while the Higgs doublets $\Phi_1$ and $\Phi_2$ remain unaffected. In addition to this, a softly broken $\mathbb{Z}_2'$ symmetry is implemented for the active Higgs fields, following which $\Phi_1$ remains unchanged whereas $\Phi_2$ undergoes the transformation $\Phi_2 \to -\Phi_2$. This specific symmetry breaking, as suggested by the Paschos-Glashow-Weinberg theorem [45], is crucial for suppressing Flavour Changing Neutral Currents (FCNCs) at tree level, ensuring the consistency of the model.

The scalar potential that remains invariant under both the gauge group of the SM and the two discrete symmetries introduced above is given as follows:

$$
\begin{aligned}
V = &-\frac{1}{2}\left\{m_{11}^2\Phi_1^\dagger\Phi_1 + m_{22}^2\Phi_2^\dagger\Phi_2 + \left[m_{12}^2\Phi_1^\dagger\Phi_2 + \text{h.c.}\right]\right\} + \frac{\lambda_1}{2}(\Phi_1^\dagger\Phi_1)^2 + \frac{\lambda_2}{2}(\Phi_2^\dagger\Phi_2)^2 \\
&+ \lambda_3(\Phi_1^\dagger\Phi_1)(\Phi_2^\dagger\Phi_2) + \lambda_4(\Phi_1^\dagger\Phi_2)(\Phi_2^\dagger\Phi_1) + \frac{1}{2}\left[\lambda_5(\Phi_1^\dagger\Phi_2)^2 + \text{h.c.}\right] \\
&+ m_\eta^2\eta^\dagger\eta + \frac{\lambda_\eta}{2}(\eta^\dagger\eta)^2 + \lambda_{1133}(\Phi_1^\dagger\Phi_1)(\eta^\dagger\eta) + \lambda_{2233}(\Phi_2^\dagger\Phi_2)(\eta^\dagger\eta) \\
&+ \lambda_{1331}(\Phi_1^\dagger\eta)(\eta^\dagger\Phi_1) + \lambda_{2332}(\Phi_2^\dagger\eta)(\eta^\dagger\Phi_2) + \frac{1}{2}\left[\lambda_{1313}(\Phi_1^\dagger\eta)^2 + \lambda_{2323}(\Phi_2^\dagger\eta)^2 + \text{h.c.}\right]
\end{aligned} \tag{2}
$$

where the $\lambda_i$'s denote the quartic coupling parameters while $m_\eta^2$, $m_{11}^2$, $m_{22}^2$ and $m_{12}^2$ are the mass-squared terms.

The two active Higgs doublets and the inert doublet under $SU(2)_L$ are parameterised as follows, respectively:

$$
\Phi_k = \begin{pmatrix} \phi_k^\pm \\ (v_k + \eta_k + iz_k)/\sqrt{2} \end{pmatrix}, \quad \eta = \begin{pmatrix} \chi^\pm \\ (\chi + i\chi_a)/\sqrt{2} \end{pmatrix}. \tag{3}
$$

Within this framework, $v_1$ and $v_2$ denote the Vacuum Expectation Values (VEVs) associated with the neutral components of the two active (pseudo)scalar doublets $\Phi_1$ and $\Phi_2$. These VEVs determine the dynamics of the Spontaneous Electro-Weak Symmetry Breaking (EWSB) mechanism of the model, giving mass to the gauge bosons and fermions (as appropriate). The $\eta$ scalar doublet, however, remains inert due to the imposition of the discrete $\mathbb{Z}_2$ symmetry. This symmetry prevents any mixing between the (pseudo)scalar states of $\eta$ and those of $\Phi_1$ and $\Phi_2$, thus ensuring that $\eta$ does not acquire a VEV or contribute to EWSB in the same way as the other doublets.

Consequently, the physical scalar spectrum arising from the two active Higgs doublets in this model is similar to the one in the pure 2HDM. This spectrum consists of four distinct Higgs particles: $h$ (neutral and CP-even), $H$ (neutral and CP-even), $A$ (neutral and CP-odd) and $H^\pm$ (charged with mixed CP), with masses $m_h, m_H, m_A$ and $m_{H^\pm}$, respectively [42, 46]. In what follows, we shall refer to the lighter CP-even state with a 95 GeV mass, $h$, as $h_{95}$ and to the heavier CP-even $H$ state with a 125 GeV mass as $h_{125}$, the former being the candidate to explain the corresponding data anomalies and latter being identified with the SM-like Higgs boson observed in experiments. Furthemore, the $A$ state is the state that we propose being behind the 650 GeV anomaly (hence, it will have a mass around such a value).

As for the inert sector, the 1(1+2)HDM introduces three additional scalar fields: $\chi$, $\chi_a$ (which are neutral) and $\chi^\pm$ (which is charged). Furthermore, we adopt the *dark democracy* approach of Refs. [47–50] in what follows, in order to reduce the number of free parameters, thus making the numerical analysis more tractable while preserving the essential features of the I(1+2)HDM. Consequently, by setting $\lambda_a = \lambda_{1133} = \lambda_{2233}$, $\lambda_b = \lambda_{1331} = \lambda_{2332}$ and $\lambda_c = \lambda_{1313} = \lambda_{2323}$, the inert squared masses can be expressed as:

$$
\begin{aligned}
m_{\chi^\pm}^2 &= m_\eta^2 + \frac{1}{2}\lambda_a v^2, \\
m_\chi^2 &= m_{\chi^\pm}^2 + \frac{1}{2}(\lambda_b + \lambda_c)v^2, \\
m_{\chi_a}^2 &= m_{\chi^\pm}^2 + \frac{1}{2}(\lambda_b - \lambda_c)v^2.
\end{aligned} \tag{4}
$$

Thus, the Higgs sector of the I(1+2)HDM is described by 12 free parameters:

$$
\begin{aligned}
\Sigma = \{\, &m_h,\, m_A,\, m_H,\, m_{H^\pm},\, m_{12}^2,\, \tan\beta,\, \sin(\beta-\alpha), \\
&m_\chi,\, m_{\chi_a},\, m_{\chi^\pm},\, m_\eta^2,\, \lambda_\eta \,\}.
\end{aligned} \tag{5}
$$

Here, $\alpha$ denotes the rotation angle in the CP-even sector, which governs the mixing between the CP-even neutral Higgs states $h$ and $H$ whereas the parameter $\beta$ (the mixing angle for both CP-odd and charged sectors) is defined as $\tan\beta = v_2/v_1$.

After enforcing the symmetries outlined above, the most general Yukawa interactions in the I(1+2)HDM resemble those of the 2HDM and the corresponding Lagrangian is given by:

$$
\begin{aligned}
\mathcal{L}_{\text{Yukawa}} &= -\overline{Q}_L Y_u \widetilde{\Phi}_u u_R - \overline{Q}_L Y_d \Phi_d d_R - \overline{L}_L Y_\ell \Phi_\ell \ell_R + \text{h.c.} \\
&\supset -\sum_{f=u,d,\ell}\left[\frac{m_f}{v}\kappa_h^f \overline{f} f h + \frac{m_f}{v}\kappa_H^f \overline{f} f H - i\frac{m_f}{v}\kappa_A^f \overline{f}\gamma_5 f A\right],
\end{aligned}
$$

where the $Y_f$'s ($f = u$, $d$ or $l$) are $3\times 3$ Yukawa matrices and $\widetilde{\Phi}_{1,2} = i\sigma_2\Phi_{1,2}^*$, with $\sigma_2$ being the Pauli matrix. In Tab. I we list all the Type-I Yukawa reduced couplings $\kappa_h^f$ and $\kappa_H^f$ of the CP-even Higgs bosons, $h$ and $H$.

| $\kappa_h^u$ | $\kappa_h^d$ | $\kappa_h^\ell$ | $\kappa_H^u$ | $\kappa_H^d$ | $\kappa_H^\ell$ |
|---|---|---|---|---|---|
| $c_\alpha/s_\beta$ | $c_\alpha/s_\beta$ | $c_\alpha/s_\beta$ | $s_\alpha/s_\beta$ | $s_\alpha/s_\beta$ | $s_\alpha/s_\beta$ |

TABLE I. The I(1+2)HDM Type-I Yukawa couplings of the neutral Higgs bosons $h$, $H$ to the up-quarks, down-quarks and leptons in the I(1+2)HDM, normalised by the corresponding SM Yukawa couplings.

### B. Theoretical and Experimental Constraints

In our random parameter scan, we retained only those points that are physically viable, i.e. consistent with both theoretical and experimental requirements. Below we provide a summary of the constraints applied to the I(1+2)HDM Type-I (see [24] for more details):

- Theoretical Constraints
  - ⋆ Perturbativity [44].
  - ⋆ Unitarity [44].
  - ⋆ Vacuum Stability [43].
- Experimental Constraints
  - ⋆ Higgs boson signal strength measurements from the LHC, implemented via `HiggsSignals-3` [51].
  - ⋆ Exclusion limits on non-SM-like Higgs bosons from direct searches at LEP, the Tevatron, and LHC, as implemented in `HiggsBounds-6` [52].
  - ⋆ Constraints on the invisible Higgs decay width (in the presence of the inert sector), as automatically included within HiggsTools [53].
  - ⋆ EW precision tests from $S$, $T$ and $U$ parameters [54], derived following the general result of [55, 56].
  - ⋆ DM searches via `micrOMEGAs` [57].
  - ⋆ Flavour constraints as evaluated using the public `SuperIso` [58] program, specifically, several Branching Ratios (BRs) have been checked: BR($B \to X_s\gamma$) [59], BR($B_s \to \mu^+\mu^-$) [60–62], BR($B \to \tau\nu$)[59], among others.

### C. The $\gamma\gamma b\bar{b}$ anomaly

Here we consider the scenario where the CP-odd scalar $A$, with a mass around 650 GeV, decays via $A \to h_{125}Z$, where the $h_{125}$ subsequently decays as $h_{125} \to \gamma\gamma$, and the $Z$ boson decays as $Z \to b\bar{b}$. For the latter decay, we have incorporated the effect of a lower cut on the invariant mass of the $Z$ decay products ($m_{b\bar{b}} > 70$ GeV) implemented in the CMS analysis of [10] through the appropriate integration of the Breit-Wigner distribution over the $b\bar{b}$ final state. This interpretation choice is both theoretically consistent and phenomenologically relevant. On one hand, the original CMS analysis [10] modelled the excess in terms of a decay of the form $X_{650} \to h_{125}Y$, where $Y$ denotes a generic spin-0 resonance. On the other hand, their event selection does not rely on spin or polarisation-sensitive observables. Instead, it targets invariant mass reconstruction and global event kinematics, yet, the phenomenological difference between a pseudoscalar decay and that of a (dominant) longitudinal vector boson is expected to have minimal impact on acceptance.

| Parameter | $m_h$ | $m_H$ | $m_A$ | $m_{H^\pm}$ |
|---|---|---|---|---|
| Scan Range | [94, 97] | 125.09 | [600, 700] | [90, $10^3$] |
| Parameter | $m_{12}^2$ | $\tan\beta$ | $s_{\beta-\alpha}$ | |
| Scan Range | [$-10^3$, $10^3$] | [0.5, 25] | [−0.4, 0.1] | |
| Parameter | $m_\eta^2$ | $m_\chi, m_{\chi_a}, m_{\chi^\pm}$ | $\lambda_\eta$ | |
| Scan Range | [$-10^5$, $10^5$] | [90, $10^3$] | [7, 12] | |

TABLE II. The scan ranges of the I(1+2)HDM Type-I parameters. (Mass (squared) are in GeV$^{(2)}$.)

With all this in mind, we also explore other possible channels that would manifest themselves over the I(1+2)HDM parameter space explaining all aforementioned anomalies, such as $A \to h_{95}Z$ and $A \to t\bar{t}$, which are indeed competitive with the decay $A \to h_{125}Z$. In particular, we will demonstrate in the following that there exist viable regions in parameter space where the BRs for these two channels are substantial and consistent with all current constraints.

## III. RESULTS AND DISCUSSIONS

Following the previous discussion, we briefly recapitulate the impact of the applied constraints on the parameter space and present our interpretation of the observed $\gamma\gamma b\bar{b}$ excess within the I(1+2)HDM Type-I. To this end, we perform a numerical scan over the free parameters in Eq. (5), as summarised in Tab. II. The resulting parameter points are subsequently tested against theoretical conditions and experimental data using a dedicated `Python` interface to the aforementioned packages or own routines to test the most recent limits.

Hereafter, for convenience, we shall use the shorthand notation for the relevant cross section: $\sigma_{\gamma\gamma b\bar{b}} = \sigma(pp \to A \to h_{125}Z \to \gamma\gamma b\bar{b})$. To start with, we found it appropriate to show the possible dependencies of such an observable on the model parameters. As can be seen from Fig. 1 (top), a low $\tan\beta \leq 5$ is necessary to accommodate the $\sigma_{\gamma\gamma b\bar{b}}$ value corresponding to the excess. Additionally, the range of $\sin(\beta-\alpha)$ that matches the $\gamma\gamma b\bar{b}$ cross section value up to $-2.5\sigma$ is relatively wide, i.e., 0.27-–0.47 (see Fig. 1 (middle)).

Regarding the bottom panel in Fig. 1, it shows that the $\sigma_{\gamma\gamma b\bar{b}}$ decreases with $m_A$ happens for phase space reasons, so that larger values of $m_A$ require larger values of the BR($h_{125} \to \gamma\gamma$). Unambiguously, though, our analysis indicates that the full mass range of $m_A$ between 600 and 700 GeV remains viable in order to account for the observed excess.

In this connection, it should be noted here that inert model parameters, while not explicitly entering the

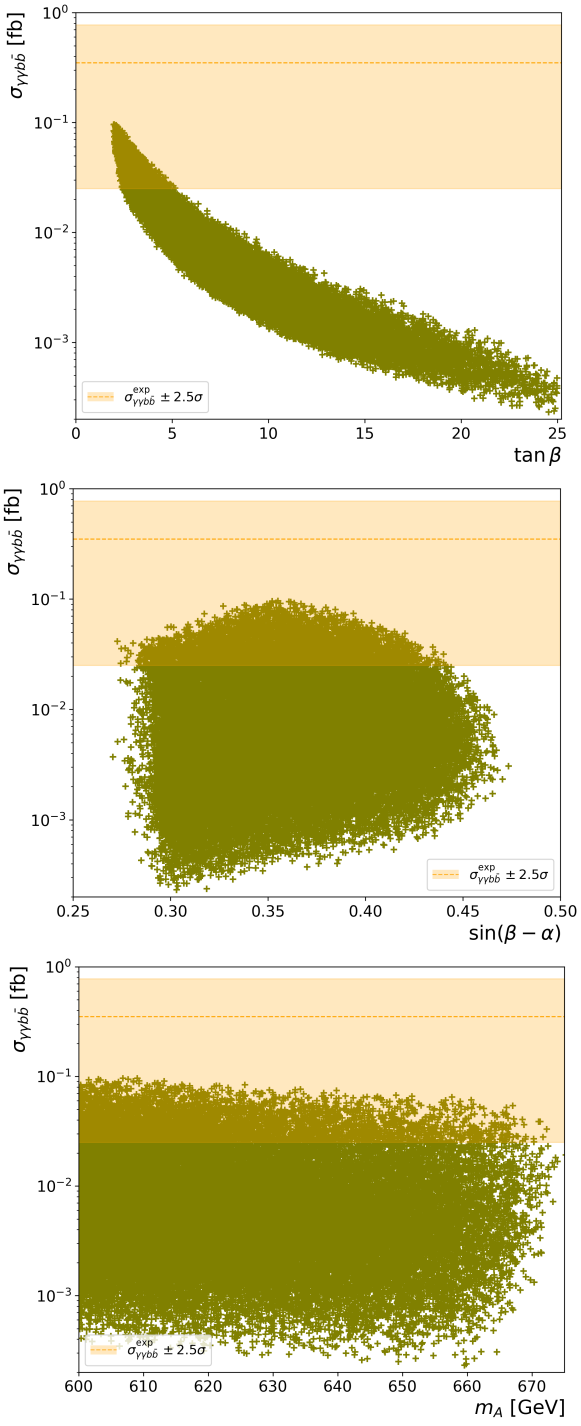


FIG. 1. The $\sigma_{\gamma\gamma b\bar{b}}$ values as function of $\tan\beta$ (top), $\sin(\beta-\alpha)$ (middle) and $m_A$ (bottom). The orange horizontal band corresponds to the value of the $\gamma\gamma b\bar{b}$ cross section consistent with the experimental measurement within $[-2.5\sigma, 0.5\sigma]$.

discussion, do affect the phenomenology of this process indirectly, in particular, the charged inert Higgs bosons with mass $100 \leq m_{\chi^\pm} \leq 500$ GeV alter the di-photon decay width of the SM-like Higgs boson, ultimately leading to $\sigma_{\gamma\gamma b\bar{b}}$ value close to the measured one. At the same time, they enter the $h_{95} \to \gamma\gamma$ decay process, enabling the I(1+2)HDM studied here to explain the 95 GeV excesses, as explained in [24].

We then show in Fig. 2 the correlations between the predicted values for $\sigma_{\gamma\gamma b\bar{b}}$ and the signal strengths $\mu_{\gamma\gamma}(h_{95})$ and $\mu_{b\bar{b}}(h_{95})$, as defined in [24], of the lighter CP-even Higgs boson $h_{95}$, for different values of $\text{BR}(A \to h_{95}\, Z)$, $\text{BR}(A \to h_{125}\, Z)$ and $\text{BR}(A \to t\bar{t})$ (ignoring the signal strength $\mu_{\tau^+\tau^-}(h_{95})$, as the excess is here more marginal in comparison).

The figure highlights the $[-2.5\sigma, 0.5\sigma]$ horizontal region in orange corresponding to the $\gamma\gamma b\bar{b}$ anomaly (as in Fig. 1) and, as a vertical band depicted in cyan, the range of values of the $\mu_{\gamma\gamma}$ (upper panel) and $\mu_{b\bar{b}}$ (lower panel) excesses within $\pm 1.5\sigma$ and $\pm 1\sigma$, respectively. From this figure, it can be seen that it is in general quite difficult to simultaneously accommodate the $\gamma\gamma b\bar{b}$ excess with the $\mu_{\gamma\gamma}(h_{95})$ and $\mu_{b\bar{b}}(h_{95})$ ones, but a non-zero overlapping region nevertheless exists.

Quite interestingly, the points most compatible with the CMS excess at 650 GeV lie within or near the experimentally allowed regions, particularly in the low-to moderate di-photon signal strength, i.e., $\mu_{\gamma\gamma}(h_{95}) \lesssim 0.2$, see Fig. 2 (top frames), and remain consistent with the $\mu_{b\bar{b}}(h_{95})$ one at $1\sigma$ level, see Fig. 2 (lower frames). For the values of BRs shown, the maximum value for $\sigma_{\gamma\gamma b\bar{b}} \approx 0.096$ fb is reached for $\text{BR}(A \to h_{95}\, Z) \approx 79.16\%$, $\text{BR}(A \to h_{125}\, Z) \approx 10.57\%$ and $\text{BR}(A \to t\bar{t}) \approx 9.86\%$. Overall, we see that, for fixed $\mu_{\gamma\gamma}(h_{95})$ and/or $\mu_{b\bar{b}}(h_{95})$, $\sigma_{\gamma\gamma b\bar{b}}$ increases inversely with $\text{BR}(A \to h_{95}\, Z)$, revealing that this decay mode dominates in the viable parameter space, with the largest BRs observed where the signal strengths $\mu_{b\bar{b}}(h_{95})$ and $\mu_{\gamma\gamma}(h_{95})$ remain consistent with experimental bounds, so that this is the key probe of the BSM scenario adopted here. Furthermore, notice that $\text{BR}(A \to t\bar{t})$ is generally not negligible, so that this channel may also be of relevance for testing the viability of the I(1+2)HDM Type-I against all the studied datasets. All this is essentially exemplifying the fact that the $A \to h_{125}Z$ mode (i.e., the apparently anomalous one) is not the only available channel for probing our scenario, so the present 650 GeV anomaly may actually be accompanied by others.

As a final point, and as already intimated, we note that the CMS Collaboration has recently carried out a dedicated analysis focusing on a possible heavy spin-0 resonance $X$ decaying into the SM-like Higgs boson and a lighter object $Y$ (again, potentially but not necessarily a spin-0 one), with the distinctive final state $\gamma\gamma\tau^+\tau^-$ [36]. They studied in particular the mass regions $m_X \approx 650$ GeV and $m_Y \approx 95$ GeV and found no significant excess. This search is thus relevant for our case as it places stringent upper limits on the production cross section times BR for the channel $pp \to A \to h_{125}Z \to \gamma\gamma\tau^+\tau^-$ in our model, ranging from 0.69 to 15 fb as a function of the $X$ mass. We have therefore accounted for this in our analysis. As shown in Fig. 3, our predictions for this process, over the region

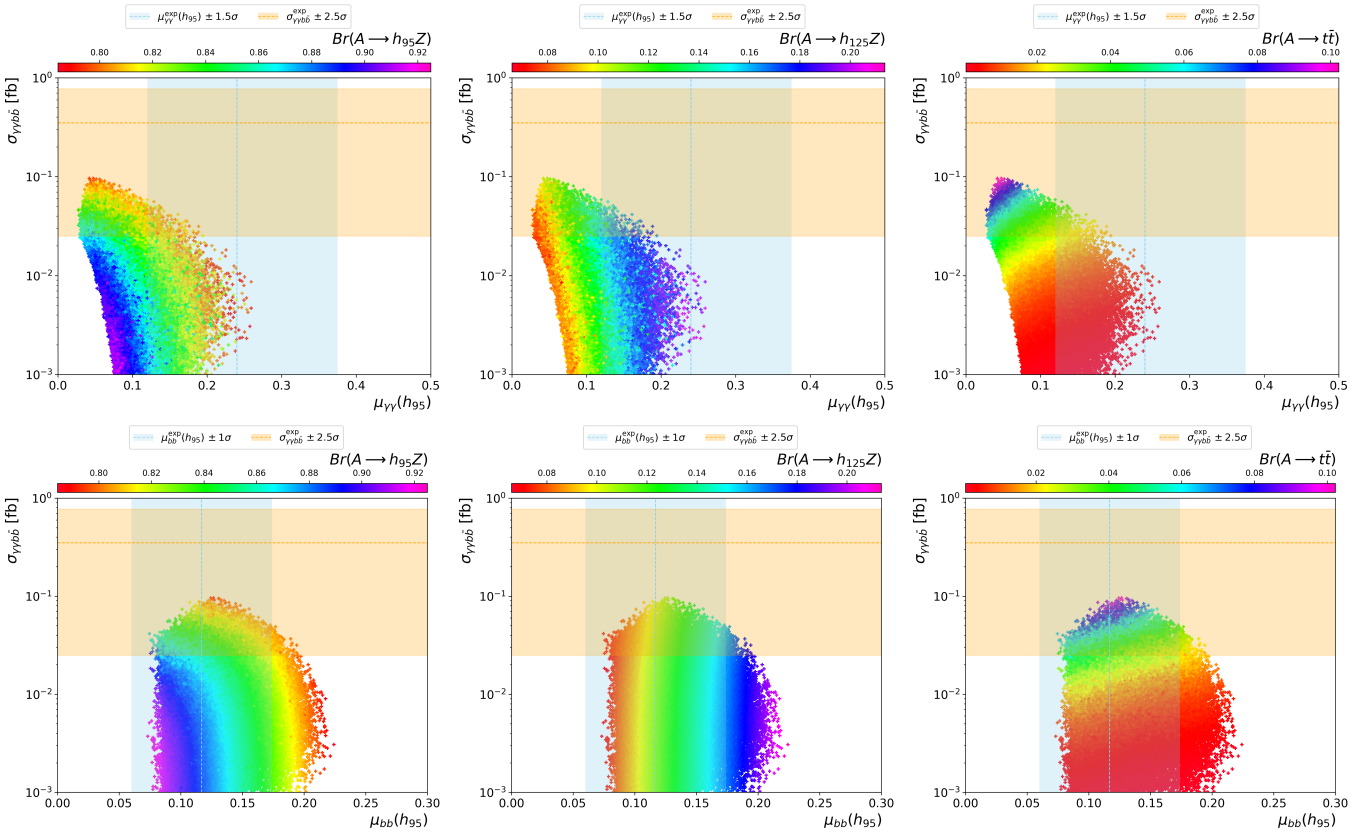

FIG. 2. The scatter plots of the production cross section $\sigma_{\gamma\gamma b\bar{b}}$, as a function of the signal strengths $\mu_{\gamma\gamma}(h_{95})$ (top) and $\mu_{b\bar{b}}(h_{95})$ (bottom). The colour coding indicates one of the following BRs: BR$(A \to h_{95})$ (left), BR$(A \to h_{125}Z)$ (middle) and BR$(A \to t\bar{t})$ (rigtht). Furthermore, in orange(cyan) horizontal(vertical) band represents the measured value of $\sigma_{\gamma\gamma b\bar{b}}$ (signal strengths $\mu_{\gamma\gamma}(h_{95})$ and $\mu_{b\bar{b}}(h)$).

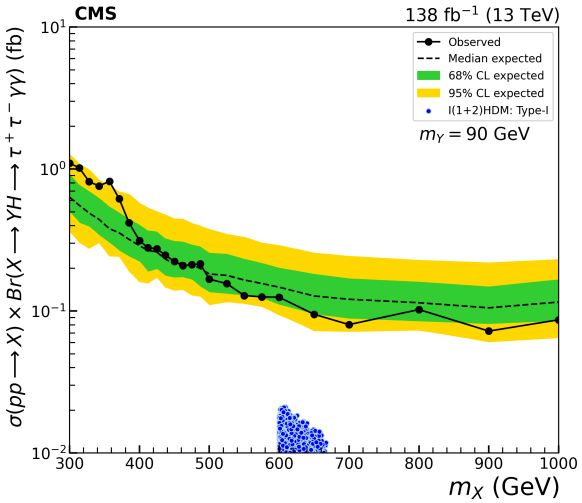


FIG. 3. The $\sigma(pp \to X \to HY \to \gamma\gamma\tau^+\tau^-)$ values as function of $m_X$ as obtained for the I(1+2)HDM points explaining the 650 and 95 GeV anomalies. Notice that, in such a scenario, one has $X = A$, $Y = Z$ and $H = h_{125}$.

of I(1+2)HDM Type-I parameter space explaining the 650 and 95 GeV anomalies simultaneously, lie below the current sensitivity lines, yet not exceedingly so. Hence, while the $\gamma\gamma\tau^+\tau^-$ final state remains unconstrained presently in our model it also represents a promising probe of the I(1+2)HDM Type-I for upcoming searches at Run 3 and the HL-LHC [63].

## IV. CONCLUSIONS

In this paper, we have tested the I(1+2)HDM Type-I as a possible theoretical scenario explaining a variety of anomalies that have recently appeared in experimental data, which origin could well be in an extended Higgs sector, with respect to the one embedded in the SM. Specifically, excesses have been seen in the search for new Higgs bosons with masses both below and above the one of the SM-like Higgs stafe detected at the LHC in 2012, with a mass of 125 GeV. In fact, anomalies have appeared around 95 GeV in analyses targeting the following processes: $e^+e^- \to Z \to h_{95}Z \to b\bar{b} + \text{jets}$) at LEP and $pp \to h_{95} \to \gamma\gamma$ and $\tau^+\tau^-$ at the LHC. Furthermore, another quite significant excess has been extracted at the LHC around 650 GeV, potentially

emerging from the process $pp \to A_{650} \to h_{125}Z \to \gamma\gamma b\bar{b}$. All such production and decay channels are present in the I(1+2)HDM and, over sizable regions of the parameter space of such a BSM scenario, they can explain all aforementioned excesses at approximately the $2\sigma$ C.L. (possibly apart from the di-tau excess, which is quite marginal, in fact). Crucially, this is made possible thanks to the presence of additional charged inert (pseudo)scalar states, a feature specific to our BSM setup (not existing, e.g., in more conventional (N)2HDMs), as they enable a perfect mapping of the 95 GeV anomaly in the di-photon channel, the most constraining one by far amongst all the discussed datasets.

In addition, alongside explaining existing anomalies, hence, through a data analysis done *a posteriori*, we have also proposed, over the parameter space of the I(1+2)HDM accommodating the various excesses, two collateral signals which should eventually appear in data. These should then be considered as *a priori* manifestations that one should expect for our theoretical framework for it to be the one underpinning Nature. The new signatures are the processes $pp \to A \to h_{95}Z$ and $pp \to A \to t\bar{t}$, which can be searched for in a variety of final states. We thus encourage the experimental Collaborations working at the current LHC and/or future HL-LHC to test such predictions, which constitute the hallmark manifestations of the I(1+2)HDM. For this purpose, we will make available upon request all our data.

## ACKNOWLEDGMENTS

SM is supported in part through the NExT Institute and STFC Consolidated Grant No. ST/L000296/1. LR would like to thank the CERN Department of Theoretical Physics for its hospitality and stimulating environment, where a part of this work was carried out.

[1] G. Aad *et al.* (ATLAS), Observation of a new particle in the search for the Standard Model Higgs boson with the ATLAS detector at the LHC, Phys. Lett. B **716**, 1 (2012), arXiv:1207.7214 [hep-ex].

[2] S. Chatrchyan *et al.* (CMS), Observation of a New Boson at a Mass of 125 GeV with the CMS Experiment at the LHC, Phys. Lett. B **716**, 30 (2012), arXiv:1207.7235 [hep-ex].

[3] R. Barate *et al.* (LEP Working Group for Higgs boson searches, ALEPH, DELPHI, L3, OPAL), Search for the standard model Higgs boson at LEP, Phys. Lett. B **565**, 61 (2003), arXiv:hep-ex/0306033.

[4] S. Schael *et al.* (ALEPH, DELPHI, L3, OPAL, LEP Working Group for Higgs Boson Searches), Search for neutral MSSM Higgs bosons at LEP, Eur. Phys. J. C **47**, 547 (2006), arXiv:hep-ex/0602042.

[5] J. Cao, X. Guo, Y. He, P. Wu, and Y. Zhang, Diphoton signal of the light Higgs boson in natural NMSSM, Phys. Rev. D **95**, 116001 (2017), arXiv:1612.08522 [hep-ph].

[6] A. Hayrapetyan *et al.* (CMS), Search for a standard model-like Higgs boson in the mass range between 70 and 110 GeV in the diphoton final state in proton-proton collisions at s=13TeV, Phys. Lett. B **860**, 139067 (2025), arXiv:2405.18149 [hep-ex].

[7] A. Tumasyan *et al.* (CMS), Searches for additional Higgs bosons and for vector leptoquarks in $\tau\tau$ final states in proton-proton collisions at $\sqrt{s} = 13$ TeV, JHEP **07**, 073, arXiv:2208.02717 [hep-ex].

[8] Search for resonances in the 65 to 110 GeV diphoton invariant mass range using 80 $\text{fb}^{-1}$ of $pp$ collisions collected at $\sqrt{s} = 13$ TeV with the ATLAS detector, (2018).

[9] Note that the best-fit mass actually differs from one channel to another, however, given the poor resolution in invariant mass of $b\bar{b}$ and $\tau^+\tau^-$ pairs, compared with to the $\gamma\gamma$ case (which is centered at 95 or so GeV), we collectively use the latter value throughout, including in our forthcoming tests of the various anomalies.

[10] A. Tumasyan *et al.* (CMS), Search for a new resonance decaying into two spin-0 bosons in a final state with two photons and two bottom quarks in proton-proton collisions at $\sqrt{s} = 13$ TeV, JHEP **05**, 316, arXiv:2310.01643 [hep-ex].

[11] G. Cacciapaglia, A. Deandrea, S. Gascon-Shotkin, S. Le Corre, M. Lethuillier, and J. Tao, Search for a lighter Higgs boson in Two Higgs Doublet Models, JHEP **12**, 068, arXiv:1607.08653 [hep-ph].

[12] R. Benbrik, M. Boukidi, S. Moretti, and S. Semlali, Explaining the 96 GeV Di-photon anomaly in a generic 2HDM Type-III, Phys. Lett. B **832**, 137245 (2022), arXiv:2204.07470 [hep-ph].

[13] R. Benbrik, M. Boukidi, S. Moretti, and S. Semlali, Probing a 96 GeV Higgs Boson in the Di-Photon Channel at the LHC, PoS **ICHEP2022**, 547 (2022), arXiv:2211.11140 [hep-ph].

[14] A. Khanna, S. Moretti, and A. Sarkar, Explaining 95 (or so) GeV Anomalies in the 2-Higgs Doublet Model Type-I, (2024), arXiv:2409.02587 [hep-ph].

[15] T. Biekötter, M. Chakraborti, and S. Heinemeyer, A 96 GeV Higgs boson in the N2HDM, Eur. Phys. J. C **80**, 2 (2020), arXiv:1903.11661 [hep-ph].

[16] S. Heinemeyer, C. Li, F. Lika, G. Moortgat-Pick, and S. Paasch, Phenomenology of a 96 GeV Higgs boson in the 2HDM with an additional singlet, Phys. Rev. D **106**, 075003 (2022), arXiv:2112.11958 [hep-ph].

[17] T. Biekötter, S. Heinemeyer, and G. Weiglein, Mounting evidence for a 95 GeV Higgs boson, JHEP **08**, 201, arXiv:2203.13180 [hep-ph].

[18] T. Biekötter, S. Heinemeyer, and G. Weiglein, The CMS di-photon excess at 95 GeV in view of the LHC Run 2 results, (2023), arXiv:2303.12018 [hep-ph].

[19] T. Biekötter, S. Heinemeyer, and G. Weiglein, 95.4 GeV diphoton excess at ATLAS and CMS, Phys. Rev. D **109**, 035005 (2024), arXiv:2306.03889 [hep-ph].

[20] A. Kundu, P. Mondal, and G. Moultaka, Indications for new scalar resonances at the LHC and a possible interpretation, (2024), arXiv:2411.14126 [hep-ph].

[21] A. Ahriche, 95 GeV excess in the Georgi-Machacek model: Single or twin peak resonance, Phys. Rev. D **110**, 035010 (2024), arXiv:2312.10484 [hep-ph].

[22] T.-K. Chen, C.-W. Chiang, S. Heinemeyer, and G. Weiglein, 95 GeV Higgs boson in the Georgi-Machacek model, Phys. Rev. D **109**, 075043 (2024), arXiv:2312.13239 [hep-ph].

[23] X. Du, H. Liu, and Q. Chang, Interpretation of 95 GeV Excess within the Georgi-Machacek Model in Light of Positive Definiteness Constraints, (2025), arXiv:2502.06444 [hep-ph].

[24] A. Hmissou, S. Moretti, and L. Rahili, Investigating the 95 GeV Higgs Boson Excesses within the I(1+2)HDM, (2025), arXiv:2502.03631 [hep-ph].

[25] J. Cao, X. Jia, Y. Yue, H. Zhou, and P. Zhu, 96 GeV diphoton excess in seesaw extensions of the natural NMSSM, Phys. Rev. D **101**, 055008 (2020), arXiv:1908.07206 [hep-ph].

[26] T. Biekötter, A. Grohsjean, S. Heinemeyer, C. Schwanenberger, and G. Weiglein, Possible indications for new Higgs bosons in the reach of the LHC: N2HDM and NMSSM interpretations, Eur. Phys. J. C **82**, 178 (2022), arXiv:2109.01128 [hep-ph].

[27] W. Li, H. Qiao, K. Wang, and J. Zhu, Light dark matter confronted with the 95 GeV diphoton excess, (2023), arXiv:2312.17599 [hep-ph].

[28] U. Ellwanger, C. Hugonie, S. F. King, and S. Moretti, NMSSM explanation for excesses in the search for neutralinos and charginos and a 95 GeV Higgs boson, Eur. Phys. J. C **84**, 788 (2024), arXiv:2404.19338 [hep-ph].

[29] J. Lian, 95 GeV excesses in the Z3-symmetric next-to-minimal supersymmetric standard model, Phys. Rev. D **110**, 115018 (2024), arXiv:2406.10969 [hep-ph].

[30] U. Ellwanger and C. Hugonie, Nmssm with correct relic density and an additional 95 GeV Higgs boson, Eur. Phys. J. C **84**, 526 (2024), arXiv:2403.16884 [hep-ph].

[31] J. Cao, X. Jia, and J. Lian, Unified interpretation of the muon g-2 anomaly, the 95 GeV diphoton, and $b\bar{b}$ excesses in the general next-to-minimal supersymmetric standard model, Phys. Rev. D **110**, 115039 (2024), arXiv:2402.15847 [hep-ph].

[32] J. Cao, X. Jia, J. Lian, and L. Meng, 95 GeV diphoton and $b\bar{b}$ excesses in the general next-to-minimal supersymmetric standard model, Phys. Rev. D **109**, 075001 (2024), arXiv:2310.08436 [hep-ph].

[33] U. Ellwanger and C. Hugonie, Additional Higgs Bosons near 95 and 650 GeV in the NMSSM, Eur. Phys. J. C **83**, 1138 (2023), arXiv:2309.07838 [hep-ph].

[34] R. Benbrik, M. Boukidi, K. Kahime, S. Moretti, L. Rahili, and B. Taki, Exploring potential Higgs resonances at 650 GeV and 95 GeV in the 2HDM Type III, Phys. Lett. B **868**, 139688 (2025), arXiv:2505.07811 [hep-ph].

[35] A. Tumasyan *et al.* (CMS), Search for a heavy Higgs boson decaying into two lighter Higgs bosons in the $\tau\tau$bb final state at 13 TeV, JHEP **11**, 057, arXiv:2106.10361 [hep-ex].

[36] A. Hayrapetyan *et al.* (CMS), Search for the nonresonant and resonant production of a Higgs boson in association with an additional scalar boson in the $\gamma\gamma\tau\tau$ final state in proton-proton collisions at $\sqrt{s} = 13$ TeV, (2025), arXiv:2506.23012 [hep-ex].

[37] A. Hayrapetyan *et al.* (CMS), Search for a new scalar resonance decaying to a Higgs boson and another new scalar particle in the final state with two bottom quarks and two photons in proton-proton collisions at $\sqrt{s} = 13$ TeV, (2025), arXiv:2508.11494 [hep-ex].

[38] And the I(1+2)HDM used here is CP-conserving, so that the decay $A \to h_{125}h_{95}$ is not possible.

[39] L. D. Landau, On the angular momentum of a system of two photons, Dokl. Akad. Nauk SSSR **60**, 207 (1948).

[40] C.-N. Yang, Selection Rules for the Dematerialization of a Particle Into Two Photons, Phys. Rev. **77**, 242 (1950).

[41] S. Moretti, Variations on a Higgs theme, Phys. Rev. D **91**, 014012 (2015), arXiv:1407.3511 [hep-ph].

[42] G. C. Branco, P. M. Ferreira, L. Lavoura, M. N. Rebelo, M. Sher, and J. P. Silva, Theory and phenomenology of two-Higgs-doublet models, Phys. Rept. **516**, 1 (2012), arXiv:1106.0034 [hep-ph].

[43] B. Grzadkowski, O. M. Ogreid, and P. Osland, Natural Multi-Higgs Model with Dark Matter and CP Violation, Phys. Rev. D **80**, 055013 (2009), arXiv:0904.2173 [hep-ph].

[44] S. Moretti and K. Yagyu, Constraints on Parameter Space from Perturbative Unitarity in Models with Three Scalar Doublets, Phys. Rev. D **91**, 055022 (2015), arXiv:1501.06544 [hep-ph].

[45] S. L. Glashow and S. Weinberg, Natural Conservation Laws for Neutral Currents, Phys. Rev. D **15**, 1958 (1977).

[46] J. F. Gunion and H. E. Haber, The CP conserving two Higgs doublet model: The Approach to the decoupling limit, Phys. Rev. D **67**, 075019 (2003), arXiv:hep-ph/0207010.

[47] V. Keus, S. F. King, S. Moretti, and D. Sokolowska, Dark Matter with Two Inert Doublets plus One Higgs Doublet, JHEP **11**, 016, arXiv:1407.7859 [hep-ph].

[48] V. Keus, S. F. King, S. Moretti, and D. Sokolowska, Observable Heavy Higgs Dark Matter, JHEP **11**, 003, arXiv:1507.08433 [hep-ph].

[49] A. Cordero-Cid, J. Hernández-Sánchez, V. Keus, S. F. King, S. Moretti, D. Rojas, and D. Sokołowska, CP violating scalar Dark Matter, JHEP **12**, 014, arXiv:1608.01673 [hep-ph].

[50] A. Cordero, J. Hernandez-Sanchez, V. Keus, S. F. King, S. Moretti, D. Rojas, and D. Sokolowska, Dark Matter Signals at the LHC from a 3HDM, JHEP **05**, 030, arXiv:1712.09598 [hep-ph].

[51] P. Bechtle, S. Heinemeyer, T. Klingl, T. Stefaniak, G. Weiglein, and J. Wittbrodt, HiggsSignals-2: Probing new physics with precision Higgs measurements in the LHC 13 TeV era, Eur. Phys. J. C **81**, 145 (2021), arXiv:2012.09197 [hep-ph].

[52] P. Bechtle, D. Dercks, S. Heinemeyer, T. Klingl, T. Stefaniak, G. Weiglein, and J. Wittbrodt, HiggsBounds-5: Testing Higgs Sectors in the LHC 13 TeV Era, Eur. Phys. J. C **80**, 1211 (2020), arXiv:2006.06007 [hep-ph].

[53] H. Bahl, T. Biekötter, S. Heinemeyer, C. Li, S. Paasch, G. Weiglein, and J. Wittbrodt, HiggsTools: BSM scalar phenomenology with new versions of HiggsBounds and HiggsSignals, Comput. Phys. Commun. **291**, 108803 (2023), arXiv:2210.09332 [hep-ph].

[54] M. Merchand and M. Sher, Constraints on the Parameter Space in an Inert Doublet Model with two Active Doublets, JHEP **03**, 108, arXiv:1911.06477 [hep-ph].

[55] M. E. Peskin and T. Takeuchi, Estimation of oblique electroweak corrections, Phys. Rev. D **46**, 381 (1992).

[56] W. Grimus, L. Lavoura, O. M. Ogreid, and P. Osland, The Oblique parameters in multi-Higgs-doublet models, Nucl. Phys. B **801**, 81 (2008), arXiv:0802.4353 [hep-ph].

[57] G. Alguero, G. Belanger, F. Boudjema, S. Chakraborti, A. Goudelis, S. Kraml, A. Mjallal, and A. Pukhov, micrOMEGAs 6.0: N-component dark matter, Comput. Phys. Commun. **299**, 109133 (2024), arXiv:2312.14894 [hep-ph].

[58] F. Mahmoudi, SuperIso v2.3: A Program for calculating flavor physics observables in Supersymmetry, Comput. Phys. Commun. **180**, 1579 (2009), arXiv:0808.3144 [hep-ph].

[59] Y. Amhis *et al.* (HFLAV), Averages of $b$-hadron, $c$-hadron, and $\tau$-lepton properties as of summer 2016, Eur. Phys. J. C **77**, 895 (2017), arXiv:1612.07233 [hep-ex].

[60] R. Aaij *et al.* (LHCb), Measurement of the $B_s^0 \to \mu^+\mu^-$ decay properties and search for the $B^0 \to \mu^+\mu^-$ and $B_s^0 \to \mu^+\mu^-\gamma$ decays, Phys. Rev. D **105**, 012010 (2022), arXiv:2108.09283 [hep-ex].

[61] R. Aaij *et al.* (LHCb), Analysis of Neutral B-Meson Decays into Two Muons, Phys. Rev. Lett. **128**, 041801 (2022), arXiv:2108.09284 [hep-ex].

[62] A. Tumasyan *et al.* (CMS), Measurement of the $B_s^0 \to \mu^+\mu^-$ decay properties and search for the $B^0 \to \mu^+\mu^-$ decay in proton-proton collisions at $\sqrt{s} = 13$ TeV, Phys. Lett. B **842**, 137955 (2023), arXiv:2212.10311 [hep-ex].

[63] F. Gianotti *et al.*, Physics potential and experimental challenges of the LHC luminosity upgrade, Eur. Phys. J. C **39**, 293 (2005), arXiv:hep-ph/0204087.